Supplemental Materials: Age-associated mitochondrial dysfunction accelerates atherogenesis

Study approval. All animal experiments, including the administration of spermidine which was approved prior to the initiation of the study, were carried out in accordance with the University of Michigan Institutional Animal Care and Use Committee.

Detailed Supplemental Methods

Mice and diet. WT young (2-3 months) and aged (18-19 months) male and female C57BL/6 mice were obtained from the National Institute on Aging rodent colony and Charles River Breeding Laboratories (stock# 027). C57BL/6 *Atg5*$^{fl/fl}$ mice were a gift from Dr. Noboru Mizushima and have been described previously.[1] *Atg5*$^{fl/fl}$ mice (C57BL/6 background) were bred to *Myh11-cre/ER*^{T2} (C57BL/6 background), which were purchased from The Jackson Laboratory (stock# 019079). *Atg5*$^{fl/fl}$*Myh11-cre/ER*^{T2} mice were treated with 3 intraperitoneal injections of tamoxifen or vehicle (corn oil) every other day to induce gene deletion then rested for 2 weeks. *Atg5*$^{fl/fl}$*Myh11-cre/ER*^{T2} mice were compared to vehicle treated litter-mate controls. *Ldlr*$^{-/-}$ mice were purchased from Jackson Laboratories (stock #002207). mtKeima, mitophagy reporter mice on the FVB/NCrl background were generously provided by Dr. Finkel.[2] These mice were aged to the indicated age under specific pathogen free conditions in the animal facility at the University of Michigan. Parkin deficient mice on the C57BL/6 background were purchased from Jackson Laboratory (stock # 006582). WT C57BL/6 controls for Parkin deficient mice were also obtained from the Jackson Laboratory. Young (5-months) and aged (21-months) UM-HET3 mice were generously provided by Dr. Richard Miller (University of Michigan). These mice are the F2 generation of (BALB/c x C57BL/6) F1 females and (C3H/He x DBA/2) F1 males.[3] These mice were aged at the Glenn Center on Aging at the University of Michigan. All mice were maintained on a 12-h light-dark cycle with free access to food and water. Sizes of experimental groups were based upon our prior studies.[4, 5]

To generate hyperlipidemic mice, an i.p., injection of recombinant adeno-associated virus 8-D377Y-murine *Pcsk9* (PCSK9-AAV) was used. The PCSK9-AAV was generated at the University of Pennsylvania Vector Core. The PCSK9-AAV was diluted in sterile saline and PCSK9-AAV or vehicle was administered i.p. at 5.0×10^9 vector genomes per gram body weight (i.e., 1.5×10^{11} vector genomes/30g mouse), similar to the intermediate dose that was previously described.[6] Mice were then rested for 1 week in their home cage and then fed a Western Diet (WD; 42% calories from fat, Teklad, catalog# 88137) or control (i.e., standard laboratory chow) low-fat diet (3% calories from fat) for 10-weeks. Spermidine (Sigma, catalog #S2626) was added to the drinking water at 3mM concentration as previously described.[7] Mice were randomly assigned to treatment with spermidine or control. The identity of spermidine group and control group was blinded to the experimenters and uncovered after the data were analyzed. UM-HET3 mice were maintained on a WD for 24-weeks. Body weights were measured at the indicated time points. Body composition analysis took place at baseline and after 10 weeks of WD (EchoMRI, Echo Medical Systems, Houston, TX, USA). A subset of aged PCSK9 WD mice were also treated with spermidine or vehicle, which was administered in water as previously described[7] for the 10-week WD feeding period.

Cholesterol, glucose, and insulin measurements. Fasting cholesterol levels were measured by colorimetric assay (Cell Biolabs, catalog# STA-384). Blood glucose was measured by glucometer (Bayer) during glucose tolerance test and insulin tolerance test, which were assessed by intraperitoneal administration of either 1.5g/body weight (kg) of glucose or 0.75U/body weight (kg) of insulin. Blood glucose levels were measured at indicated time points.

Atherosclerotic lesion analysis and histology. Mice were euthanized using isoflurane. Blood was removed by right ventricular puncture and the vasculature was perfused with ice-cold PBS. The heart was harvested and the aortic root was placed in paraformaldehyde and paraffin embedded. The aortic root was serially sectioned (6µm each). For morphometric analysis, 30 paraffin sections (6µm apart) per mouse were stained with H&E and assessed for lesion size and composition as previously described,[8] for a total distance of 360µm of the aortic sinus. For confirmation of necrotic cores, serial sections were stained with Masson's trichrome stain. The brachiocephalic artery (BCA) was chosen as a second anatomical site to assess for atherosclerosis as recommended,[9] For the BCA, histology technicians (blinded to the experimental group identity) sectioned through the artery and selected 2 sections (6µm each) at 3 anatomical points from the base at the aortic arch to the bifurcation of the carotid and subclavian artery. For the BCA, 6 sections were analyzed (6µm sections) per biological replicate. Histology processing (sectioning and staining with H&E and Masson's trichrome) was performed by the In Vivo Animal Core histology laboratory within the Unit for Laboratory Animal Medicine at the University of Michigan. Technicians in this laboratory were blinded to the experimental group identity. Total lesion size and acellular lesion area, a correlative of necrotic core size,[10] was measured using ImageJ software (NIH, USA).

Isolation of mitochondria. Mitochondria were isolated from the thoracic aorta (ThermoFisher Scientific, catalog #89801) by mincing tissues then treating with 0.3mg/mL trypsin (ThermoFisher Scientific, catalog #20233) in PBS, washing, and disrupting for 30-seconds on medium speed using a tissue homogenizer (PRO Scientific, Oxford CT, USA) and then according to manufacturer's instructions under "Option B – Protocol 1".

Immunostaining and fluorescence imaging. For immunohistochemistry, fixed paraffin-embedded sections of the aortic sinus or descending thoracic aorta were deparaffinized and rehydrated. After blocking, sections (6µm each) were incubated at room temperature for 1-2 h with Parkin (Abcam, catalog# ab77924; 1:500), Lamp1 (Santa Cruz Biotech, catalog #sc-19992), p62 (Cell Signaling Technologies, catalog #5114S), and Mac2 (Santa Cruz Biotechnology, catalog# sc-81728; 1:100). Mitotracker (Thermofisher, catalog# M22426) and Lysotracker (Thermofisher, catalog# L7528) were added to DMEM and descending thoracic aortas were incubated *ex vivo* for 1h prior to washing and imaging. Slides were used for staining with isotype controls or secondary only staining. After rinsing in PBS, slides were incubated in secondary antibodies for 1h at room temperature. Slides were counterstained in Hoechst or hematoxylin and mounted with Prolongold Diamond Antifade mountant (ThermoFisher Scientific, catalog# P36961). Two slides, each with 3-6 sections were assessed for each mouse for immunohistochemistry and immunofluorescence staining. Immunofluorescence images were captured using a Nikon A1si confocal microscope and colocalization was analyzed using

ImageJ. For imaging Parkin, p62, and Lamp1, pixel size was 188.57 nm/pixel at 60x objective. For assessment of mitophagy using mtKeima mice, the aorta was isolated and incubated with 50nM Mitotracker green (Thermofisher, catalog# M7514) for 20 minutes at 37^{O}C as our Nikon A1 microscope does not possess the filter set to excite at 462 nm and detect at the 590-650 emission range simultaneously, but is capable of excitation at 488nm and detect at the 510-560 emission range (normal FITC filter set). Using Mitotracker in conjunction with mtKeima allows one to quantify the proportion of the total mitochondria that are in the low pH environment of the lysosome. The mtKeima red fluorescent signal was obtained with excitation at 561nm and detected in the 590-650 emission range. The Mitotracker green signal was obtained by excitation at 488nm and detected within the 510-560 emission range. For the mitotracker/lysotracker images in the aortas of WT C57BL/6 mice, pixel size was 42.99 nm/pixel at 60x objective. Immunohistochemistry and H&E images were captured with an Olympus LC30 camera mounted on Olympus CX41 microscope. All data analysis was done using ImageJ and confirmed by a blinded investigator. Briefly, for Mac2 immunohistochemistry, all images were obtained with same light source at the same time. A region of interest around the total lesion area was made and a threshold used to define $Mac2^{+}$ area. The same threshold was used for all images. $Mac2^{+}$ area was normalized to total lesion area. For Parkin imaging, a region of interest was traced around the αSM-$actin^{+}$ layer of cells (i.e., the media layer) and Parkin fluorescence intensity was measured within that region of interest and averaged to the area of the region of interest. For Mitotracker and lysotracker imaging, a threshold was used to select the total area of lysotracker puncta and mitotracker puncta. Fluorescence intensity of $mitotracker^{+}$ puncta that overlapped with $lysotracker^{+}$ puncta was measured and normalized to fluorescence intensity of all $mitotracker^{+}$ puncta. Colocalized puncta were confirmed by analyzing fluorescence histograms across the puncta and confirmed by a blinded investigator. For mtKeima analysis, mean mtKeima red fluorescence intensity was normalized to mean Mitotracker green fluorescence intensity.

Mitochondrial DNA copy number and breaks. The ascending aorta, aortic arch, and descending thoracic aorta was harvested and flash-frozen. DNA was isolated using DNeasy Blood and Tissue Kit (Qiagen, catalog# 69504). The ratio of mitochondrial DNA copy number to nuclear DNA copy number was determined by real-time PCR (Detroit R&D, catalog #MCN3) according to manufacturer's instructions using 2ng of DNA samples. The fold-change was calculated using $\Delta\Delta$Ct method and normalized to the young control group. Mitochondrial DNA breaks were assessed using real-time PCR mitochondrial DNA damage analysis kit (Detroit R&D, catalog# DD2M) according to manufacturer's instructions. DNase I (Sigma, catalog #DN25) was added to enzymatically digest the aortic DNA to assess if this reduced the PCR amplification signal of the 8.2kb mtDNA product.

Respirometry of aortas. The ascending aorta, aortic arch, and descending thoracic aorta were dissected, cleaned of perivascular fat, and placed in ice-cold respiration medium consisting of 0.5mM EGTA (Sigma, catalog# E4378), 3mM $MgCl_2$ 6 hexahydrate (Sigma, catalog# M9272), 60mM lactobionic acid (Sigma, catalog# 153516), 20mM taurine (Sigma, catalog# T0625), 10mM KH_2PO_4 (Sigma, catalog# P5655), 20mM HEPES (ThermoFisher Scientific, catalog# 15630080), 110mM D-sucrose (Sigma, catalog# S0389), and 1g/L bovine serum albumin at pH

7.1.[11] High-resolution oxygen consumption measurements were conducted in 2mL of MiR05 using the Oroboros Oxygraph 2k (O2k; Oroboros Instruments, Innsbruck, AT). Polarographic oxygen measurements were acquired at 2 second intervals with the steady state rate of respiration calculated from a minimum of 30 data points and expressed as pmol s^{-1} per mg wet weight. All respiration measurements were conducted at 37^{o}C in a working range [O2] of ~200-100µM. Respiration was measured with sequential titrations of: 1.25mM ADP (CalBiochem, catalog# 117105), 2mM malate (Sigma, catalog# M1000), 5mM pyruvate (Sigma, catalog# P2256), 10mM glutamate (Sigma, catalog# G1626), 10mM succinate (Sigma, catalog# S2378), 0.5µM CCCP (Sigma, catalog# C2759), 0.5µM rotenone (Sigma, catalog# R8875), 40mM succinate, and 2.5µM antimycin-A (Sigma, catalog# A8674).

Ex Vivo Aorta Culture. For autophagic flux assays, the ascending aorta, aortic arch, and descending thoracic aortas were cleaned and harvested from young (3-month) and aged (18-month) old mice. Aortas were immediately split in 2 pieces (superior and inferior) and randomized into either DMEM+0%FBS (starved) or DMEM+20%FBS (control) for 2-hours. Aortas were rinsed 3x in PBS and flash frozen. For FCCP titration assays, the ascending aorta, aortic arch, and descending thoracic aortas from aged (18-month) old mice were cleaned and harvested. Aortas were split into 5 individual pieces and cultured in increasing concentrations of FCCP (i.e., the 5 pieces were randomized to culture media containing: 0µm, 0.0001µm, 0.01µm, 1.0µm, or 100µm FCCP) in DMEM+10%FBS. Tissues were cultured for 2h in media with FCCP and then washed 3x in PBS and flash frozen. For respirometry of *ex vivo* cultured aortas, the ascending aorta, aortic arch, and descending thoracic aorta was cultured in DMEM+10% FBS supplemented with 1.0µm FCCP or control (100% ethanol) for 2h then washed 3x prior to beginning respirometry experiments. Aortas were cultured with 10ng/ml recombinant IL-6 (PeproTech, catalog #216-16), 5µg/ml of anti-IL-6 monoclonal antibody (R&D Systems, catalog #MAB406, clone MP5-20F3), or isotype control antibody for 2h. After 2h of IL-6, anti-IL-6 antibody, or control antibody, the tissue was washed 3x with PBS. (Doses of recombinant IL-6 and anti-IL-6 were established in preliminary dose-titrating experiments). Then the tissue was either assessed for oxygen consumption rate via respirometry detailed above, or immunoblotting performed as detailed below.

Immunoblotting. The ascending aorta, aortic arch, and descending thoracic aorta was harvested, flash-frozen, and homogenized for 30s in lysis buffer (Thermofisher Scientific, catalog# 78510) with 1% protease inhibitor cocktail (Sigma, catalog# P8340) and 1% phosphatase inhibitor cocktail (Sigma, catalog# P5726) using tissue homogenizer (PRO Scientific, Oxford CT, USA). Immunoblotting of mitochondria was performed as with other tissues. Tissue lysates were electrophoresed on 4-12% gradient SDS-polyacrylamide gels and transferred to 0.20µm PVDF membranes (ThermoFisher Scientific, catalog# IB401001). Isolated mitochondria were loaded onto the gel along with whole aortic lysates to demonstrate the purity of the isolation and isolated mitochondrial protein expression was normalized to the mitochondrial loading control, CoxIV. Blots were blocked in PBS + 0.1% Tween-20 + 5% BSA for 2 h at room temperature or 4^{o}C overnight. Membranes were then incubated for 1h at room temperature with primary antibodies against Parkin (Abcam, catalog# ab77924; 1:500), PINK1 (Abcam, catalog# ab23707; 1:500), TLR9 (Santa Cruz Biotechnology, catalog# sc-52966; 1:250),

MyD88 (Cell Signaling Technology, catalog# 4283S; 1:1000), IL-6 (Cell Signaling Technology, catalog# 12912; 1:500), total OXPHOS rodent antibody cocktail (complex V alpha subunit, complex III core protein II, complex II subunit SDHB; Abcam, catalog# ab110413, 1:1000), LC3 (Cell Signaling, catalog# 4108, 1:1000), p62 (Cell Signaling, catalog# 5114S, 1:1000), Lamp1 (Santa Cruz Biotechnology, catalog# sc19992), Nix (Santa Cruz Biotechnology, catalog# sc-166332), ATG5 (Abcam, catalog# ab108327), CoxIV (1:1000, Abcam, catalog #ab16056), ubiquitinylated proteins (EMB Millipore, catalog#04-263), and β-actin (Abcam, catalog# ab8226; 1:1000). After washing in PBS + 0.1% Tween-20, membranes were incubated in secondary antibodies for 30min (Abcam, catalog# ab205718 and ab205719; 1:5000-1:10000) then illuminated with chemiluminescent substrate (ThermoFisher Scientific, catalog# 34577) using a BioRad ChemiDoc (Hercules, CA, USA).

Metabolic cages. Metabolic cage experiments were performed by the Michigan Mouse Metabolic Phenotyping Center according to National Mouse Metabolic Phenotyping Center guidelines. Oxygen consumption (VO_2), carbon dioxide production (VCO_2), spontaneous motor activity and food intake were measured using the Comprehensive Laboratory Monitoring System (CLAMS, Columbus Instruments), an integrated open-circuit calorimeter equipped with an optical beam activity monitoring device. Mice were weighed each time before the measurements and individually placed into the sealed chambers (7.9"x4"x5") with free access to food and water. Measurements were carried out continuously for 72h. During this time, animals were provided with food and water through the equipped feeding and drinking devices located inside the chamber. The amount of food of each animal was monitored through a precision balance attached below the chamber. VO_2 and VCO_2 in each chamber were sampled sequentially for 5s in a 10min interval and the motor activity was recorded every second in X and Z dimensions. The air flow rate through the chambers was adjusted at the level to keep the oxygen differential around 0.3% at resting conditions. Respiratory exchange ratio (RER), was calculated as VCO_2/VO_2. Total energy expenditure, carbohydrate oxidation, and fatty acid oxidation can be calculated respectively based on the values of VO_2, VCO_2, and the protein breakdown which estimated from urinary nitrogen excretion using the following equations: fat oxidation=$(1.69)(VO_2)-(1.69)(VCO_2)-(2.03)(n)$ and glucose oxidation=$(4.57)(VCO_2)-(3.23)(VO_2)-(2.60)(n)$.[12]

ELISAs. Animals were fasted overnight for 16h before plasma collection. Insulin (Chrystal Chem, catalog# 90080), Adiponectin (ThermoFisher Scientific, catalog# KMP0041), and Leptin (ThermoFisher Scientific, catalog# KMC2281) ELISAs were performed according to manufacturer instructions.

Flow cytometry. Blood was harvested from animals via the central tail artery and the red blood cells were lysed via addition of 3.6mL de-ionized water immediately followed by .4mL 10X PBS, resulting in 1X PBS. Cells were then centrifuged for 5 minutes at 400xG and then the supernatant was poured off. Pellets were washed again then resuspended with 1:50 FCγR block (Biolegend) in 50µl flow cytometry buffer (FACS buffer), 1× PBS containing 5% FBS and 5mM EDTA. Cells were incubated for 15 minutes and then an additional 50µL FACS buffer containing antibody cocktail was added. Cells were incubated at room temperature for 20 minutes with

antibody cocktail containing anti-MHC Class II (I-A/I-E) (PerCP-eFluor710, Invitrogen, catalog# 46-5321-82), anti-CD11b (BV510, Biolegend, catalog# 101263), anti-Ly-6c (AF488, Invitrogen, catalog# 53-5932-82), and anti-Ly-6g (BV421, Biolegend, catalog# 127627). Cells were then fixed and permeabilized (Fix & Perm Cell Kit, ThermoFisher, catalog# GAS004) according to manufacturer's instructions. Briefly, 100µl reagent A (fixation) was added after antibody incubation for 10 minutes, then washed with 3mL FACS buffer, then 100µl reagent B (permeabilization) along with anti-Parkin (AF647, Santa Cruz Biotechnology, catalog# sc-32282) or isotype control anti-IgG (AF647, Santa Cruz Biotechnology, catalog# sc24638). Cells were incubated for 20 minutes. Cells were washed with 1mL FACS buffer 2 times and then resuspended in 200µl FACS buffer. Flow cytometry was acquired with a Coulter Cytoflex and data were analyzed with FlowJo software. The gating strategy used is demonstrated in Supplemental Figure 11G. Parkin median fluorescence intensity was calculated for Ly-6c^{hi} monocytes, Ly-6c^{lo} monocytes, and neutrophils and subtracted from anti-IgG isotype control.

Statistics. All results are presented as mean ±standard error of the mean (SEM). Normality was determined using Shapiro-Wilk test. Nonparametric tests were used for data that are not normally distributed. Data with 1 independent variable (i.e., age) were analyzed using Student's *t* test or Mann-Whitney U-test (non-parametric). When more than 1 independent variable were analyzed (i.e., age and diet or repeated measures), one-way ANOVA (or Kruskal-Wallis test) or 2-way ANOVA with multiple comparisons were used. Specific statistical tests and *P values* are denoted in figure legends. The study did not correct for multiple testing across the whole study. Two-sided *P values* were used and values <0.05 were considered significant. Graphpad Prism was used to generate figures and for statistics.

Supplemental Material

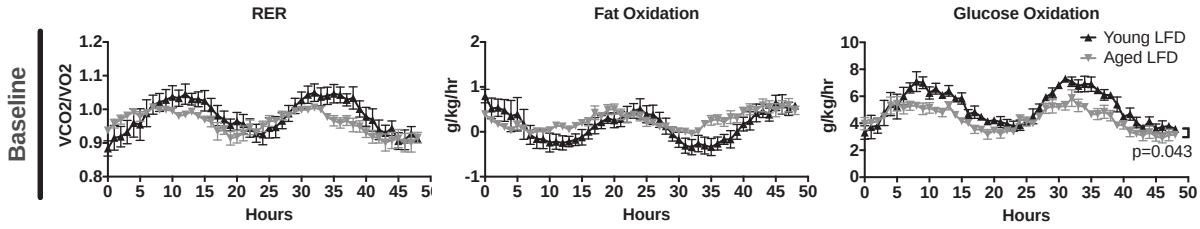

Online Figure I: Young and aged mice have similar whole-body metabolism. Young and aged LFD-fed WT mice were housed in metabolic cages for 72 h. Mice were acclimated in the first 24h and the final 48h were analyzed. (**A**) RER, fat oxidation, and glucose oxidation of young and aged WT-LFD fed mice (n=5 young and 6 aged mice per group). All results are presented as mean ±SEM. Calculations for RER, fat oxidation, and glucose oxidation are detailed in Methods. Statistics are based on Mann-Whitney U-tests comparing AUC. LFD=low-fat diet, RER=respiratory exchange ratio.

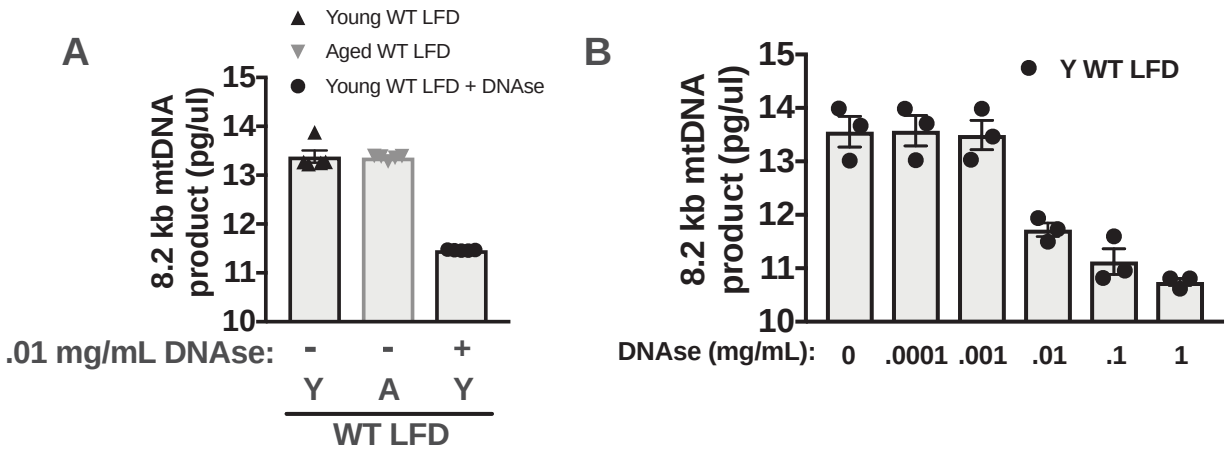

Online Figure II: Measurement of mtDNA breaks in the aorta of young and aged WT mice during normolipidemia

(A) Real-time quantitative PCR of total aortic DNA from young and aged mice to detect breaks in an 8.2kb strand of mitochondrial DNA. Aortic DNA from young aortas were treated with DNAse at 0.1 mg/mL dose. (**B)**: Aortic DNA was isolated from young mice fed a low-fat diet and treated with increasing doses of DNAse. PCR for the 8.2Kb mtDNA product was subsequently run. Each data point represents a biological replicate.

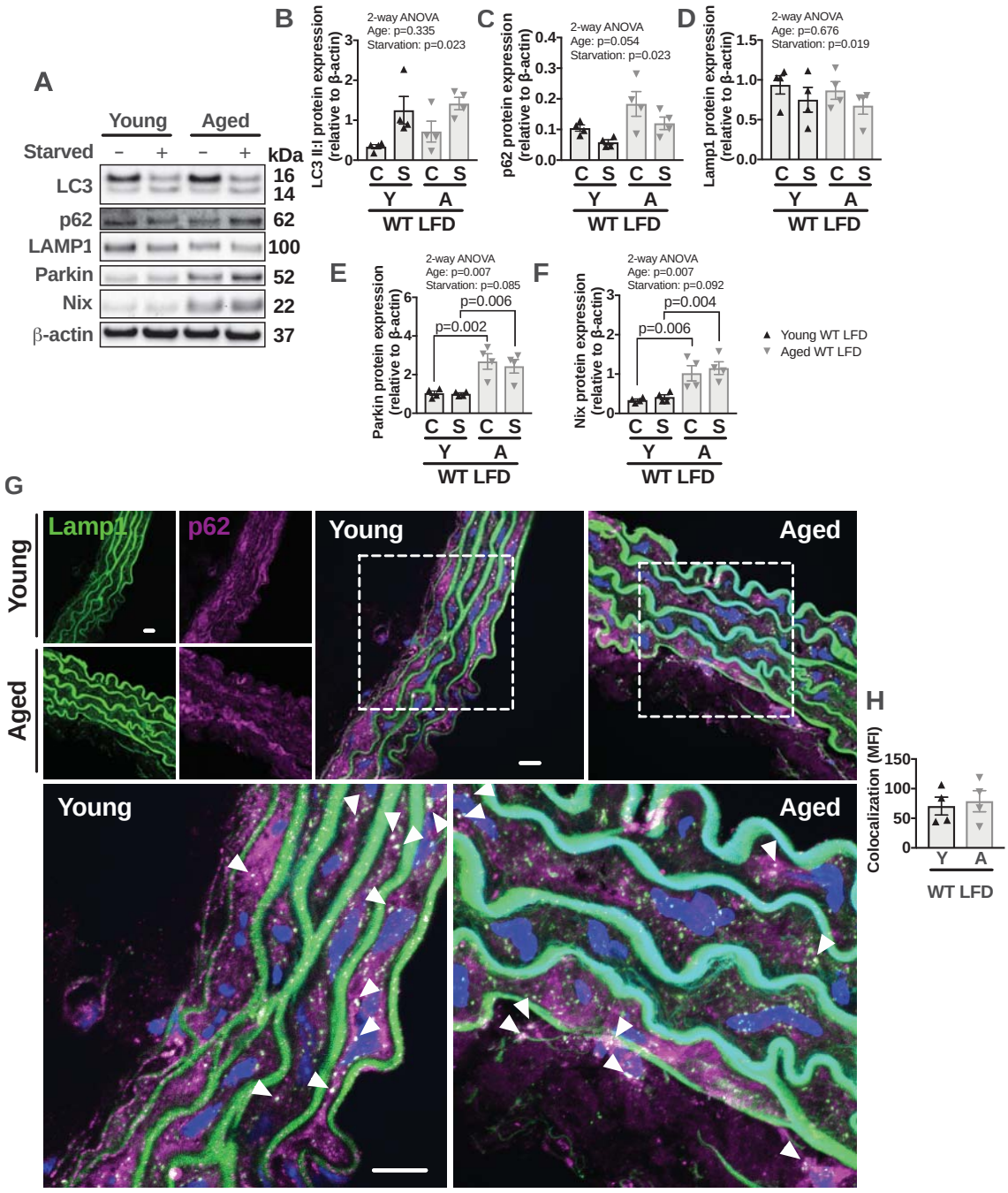

Online Figure III: Similar level of autophagy in the aortas of young and aged normolipidemic mice. (**A**) Thoracic aortas from young or aged WT, LFD-fed mice were harvested and cultured in DMEM+0%FBS (starvation) or DMEM+20%FBS (control) for 2h prior to flash-freezing for protein immunoblotting. Membranes were blotted against LC3 (LC3I is upper band, LC3II lower band), p62, LAMP1, Parkin, Nix, and β-actin. (**B**-**F**) Quantification of immunoblots. Thoracic aortas from young or aged WT, LFD-fed mice were harvested and then assessed by fluorescent microscopy for Lamp1 and p62. (**G**) Fixed frozen aortic sections (6μm) were stained with primary antibodies against Lamp1 and p62, secondary antibodies, and nuclei were stained with hoechst. White arrowheads demonstrating colocalized puncta, appear white. (**H**) Quantification of p62 puncta mean fluorescence intensity that colocalized with Lamp1 puncta. Scale bars: 10μm. 2-way ANOVA with Sidak's post-hoc test for **B**-**F**. Mann-Whitney U-test for **H**. Each data point represents a biological replicate. C = control, S = starved.

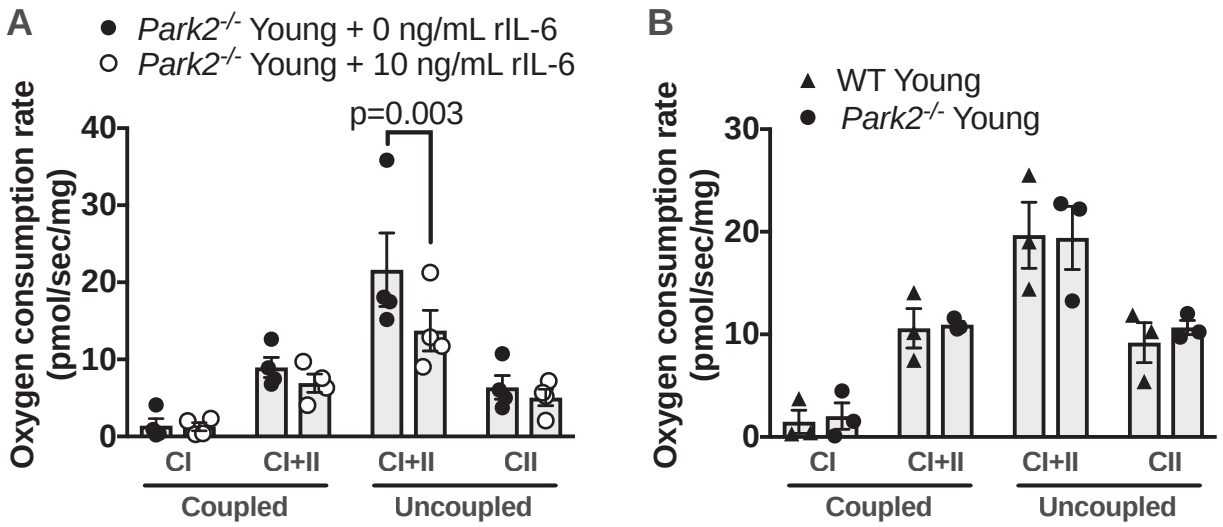

Online Figure IV. (**A**) Thoracic aortas from young WT and *Park2*$^{-/-}$ (Parkin deficient) normolipidemic mice were incubated in DMEM+10%FBS for 2 h followed by 3 washes prior to respirometry experiments following the same protocol from **Figure 1A**. (**B**) Thoracic aortas from young *Park2*$^{-/-}$ (Parkin deficient) mice were incubated in DMEM+10%FBS with either 0 or 10ng/ml of IL-6 for 2h and then OCR was assessed per **Figure 1A**. Data are maximal aortic OCR with substrates for complex I and I+II coupled OXPHOS and maximal complex I+II and II uncoupled OCR. Each data point represents a biological replicate. Two-way ANOVA with Sidak's post-hoc test. All results are presented as mean ±SEM. WT=wild-type, *Park2*$^{-/-}$=Parkin deficient, CI=complex I, CII=complex II.

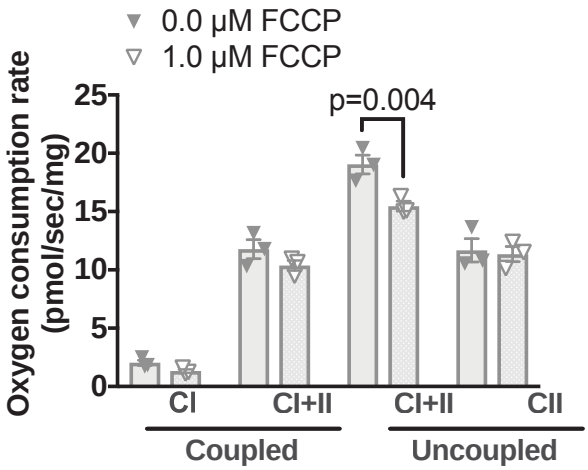

Online Figure V. FCCP reduces OCR in aortas of aged normolipidemic mice. Aortas from 18-month old WT C57BL/6 mice were harvested and cultured in DMEM+10% FBS either supplemented with 1µm FCCP or vehicle (100% ethanol) for 2 h followed by 3 washes prior to respirometry experiments following the same protocol from **Figure 1A**. Data are maximal aortic OCR with substrates for complex I and I+II coupled OXPHOS and maximal complex I+II and II uncoupled OCR. Two-way ANOVA with Sidak's post-hoc test. All results are presented as mean ±SEM. Each point is a biological replicate. CI=complex I, CII=complex II.

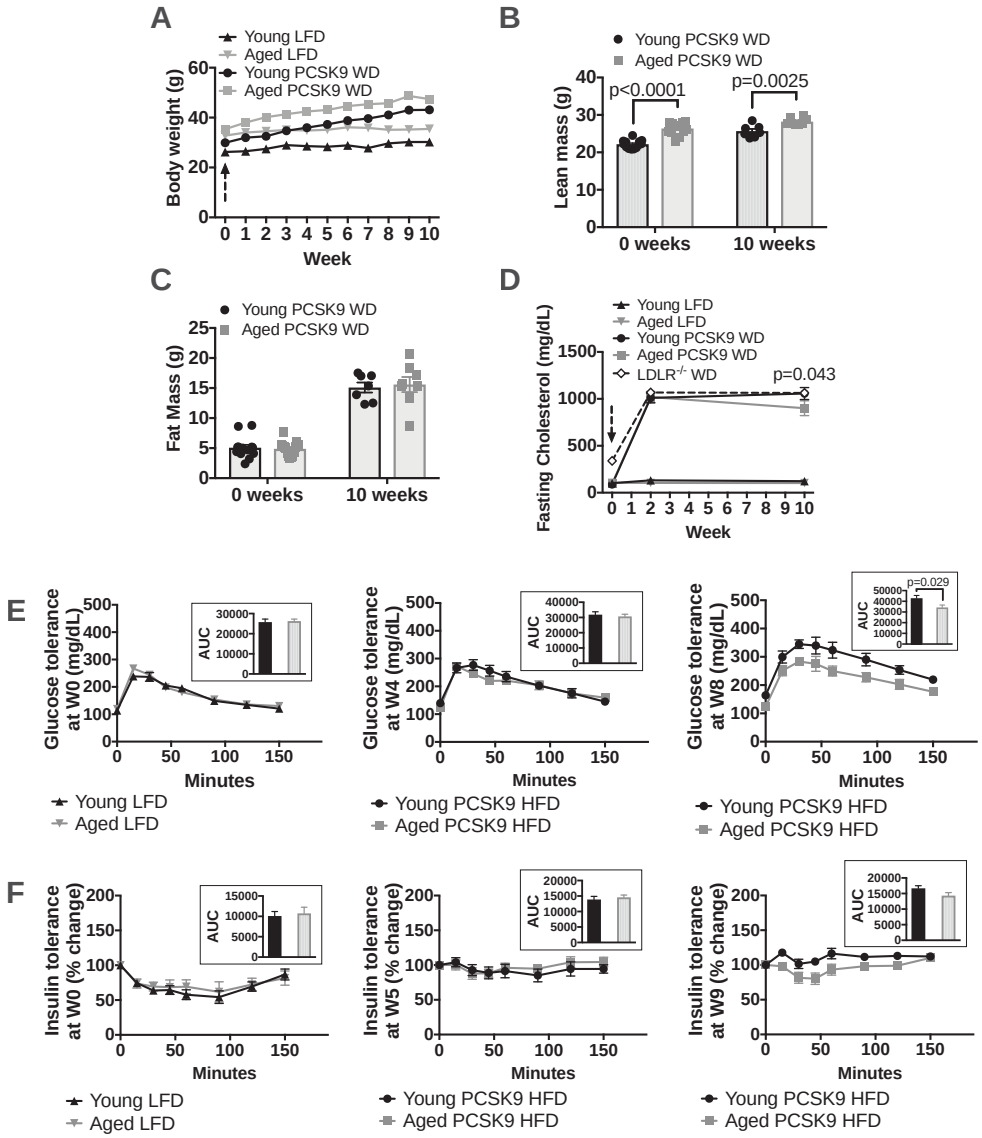

Online Figure VI: Similar induction of hypercholesterolemia in young and aged WT mice. Body weight, body composition, fasting cholesterol, glucose tolerance, and insulin tolerance were measured at baseline and over the 10-week WD feeding period in young and aged C57BL/6 WT mice. (**A**) Body weight in grams (n=7 young WT-LFD, 5 aged WT-LFD, 26 young PCSK9-WD, and 27 aged PCSK9-WD mice). Arrow indicates start of WD-feeding or LFD-fed littermate controls. (**B**) Lean mass, including organ weight, was determined by Echo-MRI. (**C**) Fat mass was determined by Echo-MRI (n=7 young PCSK9-WD and 8 aged PCSK9-WD mice for **B** and **C**). (**D**) Fasting total cholesterol was quantified from plasma via colorimetric assay (n=4 young-LFD, 2 aged-LFD, 16 young PCSK9-WD, 14 aged PCSK9-WD, and 4 young *Ldlr*$^{-/-}$-WD mice). Arrow indicates start of WD-feeding or LFD-fed littermate controls. Statistical significance is between young and aged PCSK9-WD groups at 10-week time point by Mann-Whitney U-test. (**E**) Glucose tolerance tests were performed at baseline, 4, and 8-weeks after WD-feeding (n=7 young and 7 aged PCSK9-HFD mice). (**F**) Insulin tolerance tests were performed at baseline and 5 and 9-weeks after WD-feeding (n=7-10 young and 7-9 aged PCSK9-HFD mice). All mice are WT except *Ldlr*$^{-/-}$ mice. All results are presented as mean ±SEM. Mann-Whitney U test for **E** and **F** AUC. Unpaired *t*-test were used for **B** and **C**. PCSK9-WD denotes mice that received *Pcsk9* gene transfection and then fed WD. LDLR=LDL receptor, LFD=low-fat diet, PCSK9=proprotein convertase subtilisin/kexin 9, WD=western diet.

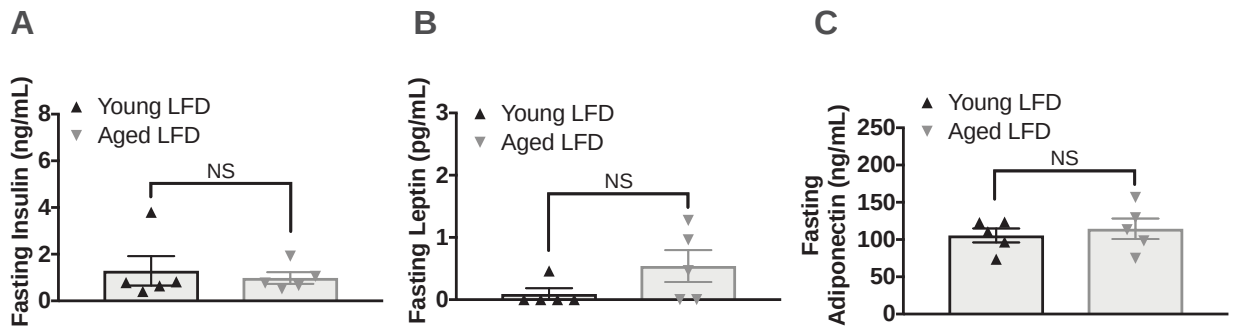

Online Figure VII: Young and aged mice have similar fasting insulin, leptin, and adiponectin plasma levels. Fasting plasma was collected from young and aged WT LFD-fed mice. (**A**) Fasting plasma insulin. (**B**) Fasting plasma leptin. (**C**) Fasting plasma adiponectin. n=5 mice per group. All results are presented as mean ±SEM. LFD=low-fat diet. Each data point represents a biological replicate.

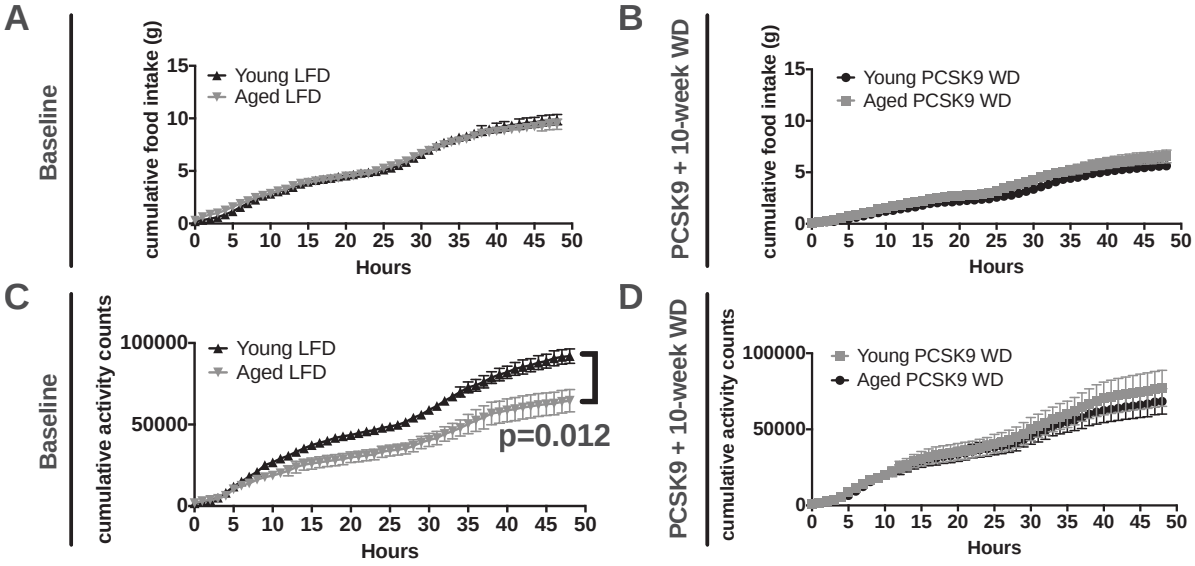

Online Figure VIII: Young and aged mice have similar food intake and activity. Mice were housed in metabolic cages for 72 h. Mice were acclimated in the first 24-h and the final 48 h were analyzed. (**A**) Food intake for young and aged WT-LFD fed mice. (**B**) Food intake for young and aged PCSK9-WD mice. (**C**) Activity counts for young and aged WT-LFD fed mice. (**D**) Activity counts for young and aged PCSK9-WD mice. n=5 young and 6 aged mice per group. All results are presented as mean ±SEM. Statistics are based on Mann-Whitney U-tests comparing AUC. LFD=low-fat diet, PCSK9=proprotein convertase subtilisin/kexin 9, WD=western diet.

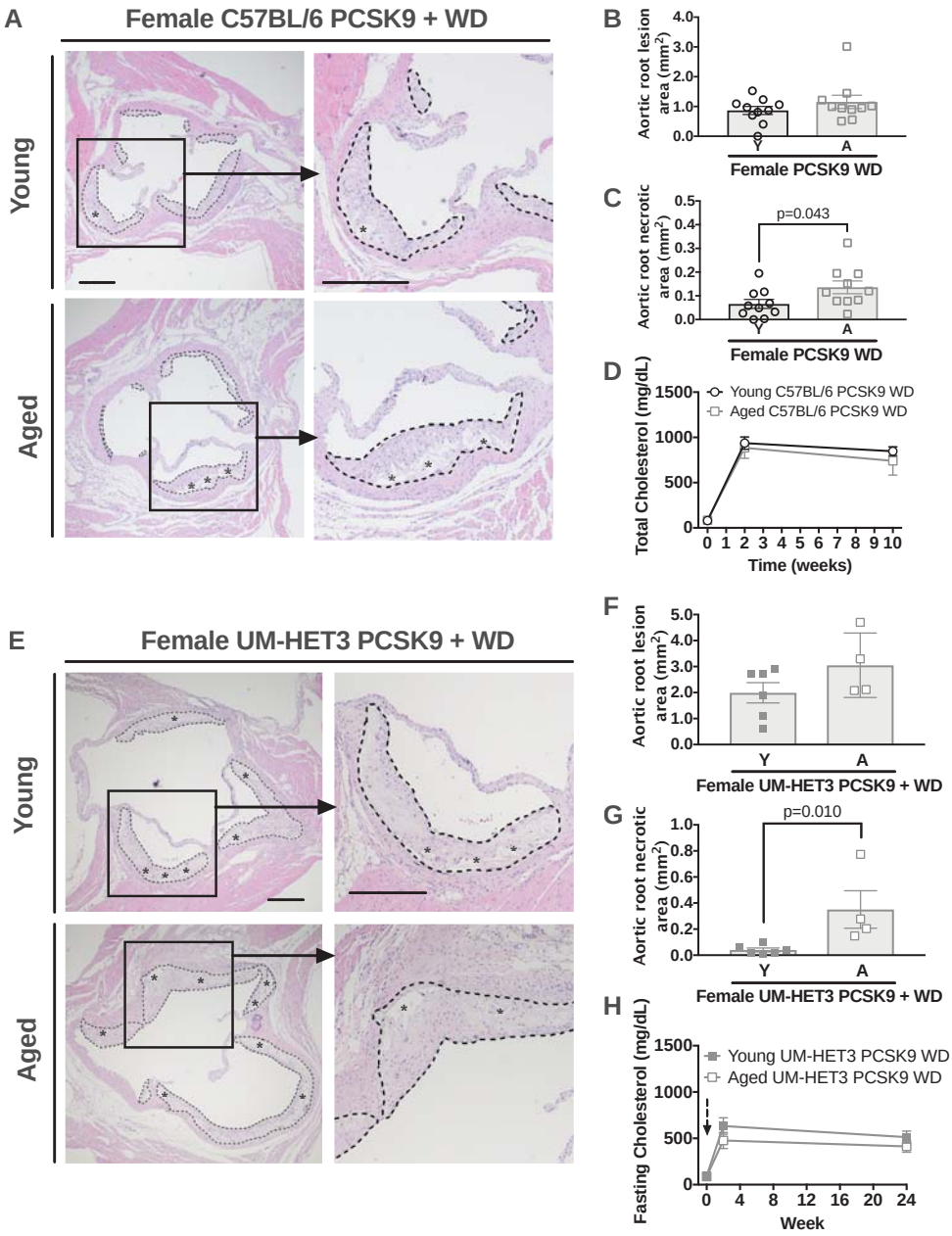

Online Figure IX: Aged female atherosclerotic mice have larger necrotic cores within atherosclerotic plaques than young mice. Female C57BL/6 mice (**A-D**) or Female UM-HET3 mice (see METHODS) (**E-H**): were maintained on a LFD until 3-months or 18-months (for C57BL/6) or 5-months or 21-months (for UM-HET3) and were transfected with PCSK9-AAV and diet was switched to WD for 10-weeks (C57BL/6) or 24-weeks (UM-HET3) until euthanasia and sectioning the aortic root. (**A** & **E**) Cross sections of the aortic root showing total lesion area, outlined in dashed lines, and necrotic cores, denoted by asterisks. Scale bar: 100µm. (**B** & **F**) Quantification of total plaque size. (**C** & **G**) Quantification of necrotic core size. (**D** & **H**) Fasting total cholesterol at indicated time-points. N=6 young and 5 aged C57BL/6 and N=6 young and 5 aged UM-HET3 female mice for cholesterol assay. Each point is a biological replicate. For atherosclerotic plaque and necrotic area, each biological replicate is the sum of 30 serial sections, 6µm per section. All results are presented as mean ±SEM. Mann-Whitney U-tests. PCSK9=proprotein convertase subtilisin/kexin 9, WD=western diet.

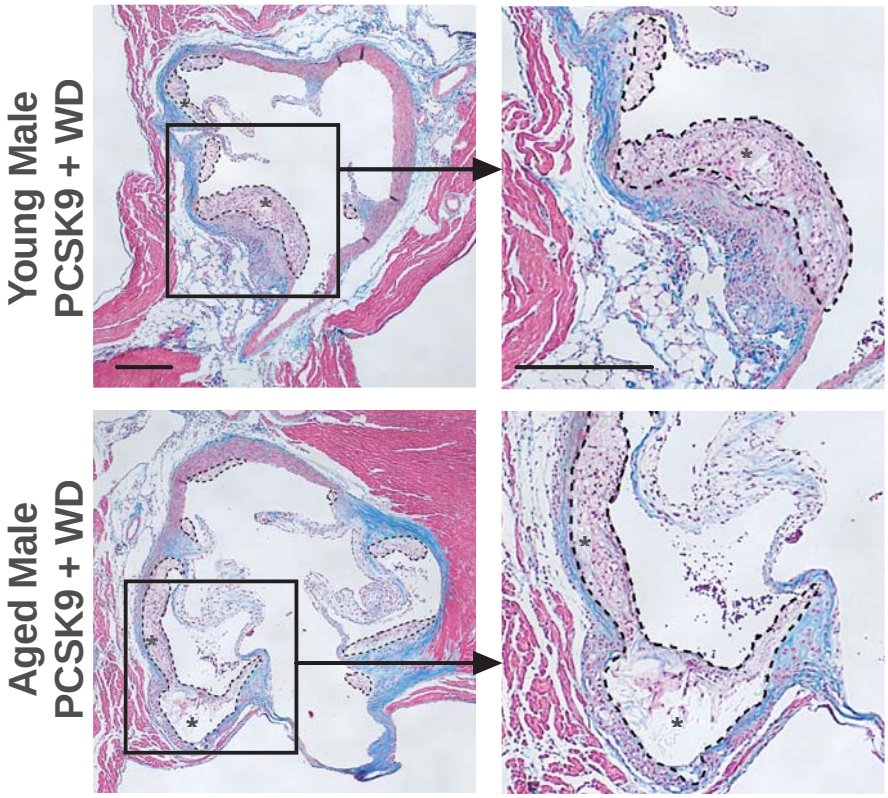

Online Figure X: Aged male atherosclerotic mice have larger necrotic cores within atherosclerotic plaques than young mice. Male C57BL/6 mice were maintained on a LFD until 3-months or 18-months and were transfected with PCSK9-AAV and diet was switched to WD for 10-weeks until euthanasia and sectioning the aortic root. Representative images of Masson's Trichrome stain on serial sections from **Figure 5A**. Cross sections of the aortic root show total lesion area, outlined in dashed lines, and necrotic cores, denoted by asterisks. Scale bar: 100µm. 6µm per section. PCSK9=proprotein convertase subtilisin/kexin 9, WD=western diet.

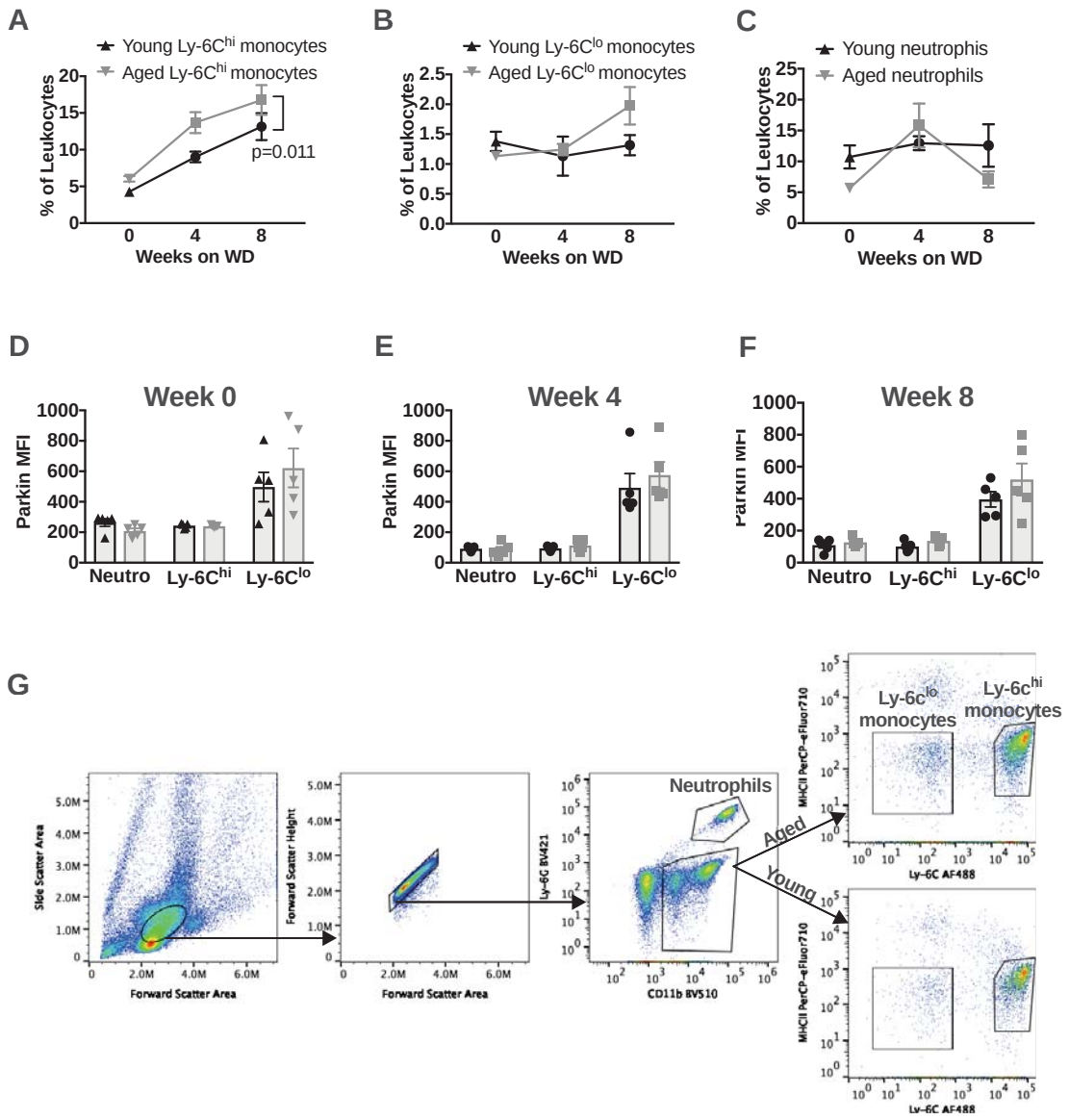

Online Figure XI: Mice exhibit increased inflammatory monocytosis during HFD with aging. Parkin levels within monocytes are similar between young and aged mice before and after a HFD. Young and aged mice were maintained on a LFD or were transfected with PCSK9-AAV and diet was switched to WD for 8 weeks. At week 0, 4 and 8 of the diet the mice were bled and the proportion of circulating monocytes and neutrophils were enumerated by antibody staining coupled to flow cytometry. (**A-C**) Cells were sub divided into inflammatory (Ly6-C^{hi}) and patrolling (Ly-6C^{lo}) monocytes and neutrophils (Ly-6G^{hi}). (**D-F**) Parkin (conjugated to AF647) expression within each of the cells assessed in A-C were evaluated for the expression for Parkin by intracellular staining as described in methods. Parkin median fluorescence intensity was calculated for Ly-6c^{hi} monocytes, Ly-6c^{lo} monocytes, and neutrophils and subtracted background fluorescence obtained from the anti-IgG isotype control. 2-way ANOVA with Sidak's post-hoc test. **G:** Gating strategy. MFI=median fluorescent intensity. All data are from the same groups of mice. Each data point is a biological replicate. PCSK9=proprotein convertase subtilisin/kexin 9, WD=western diet.

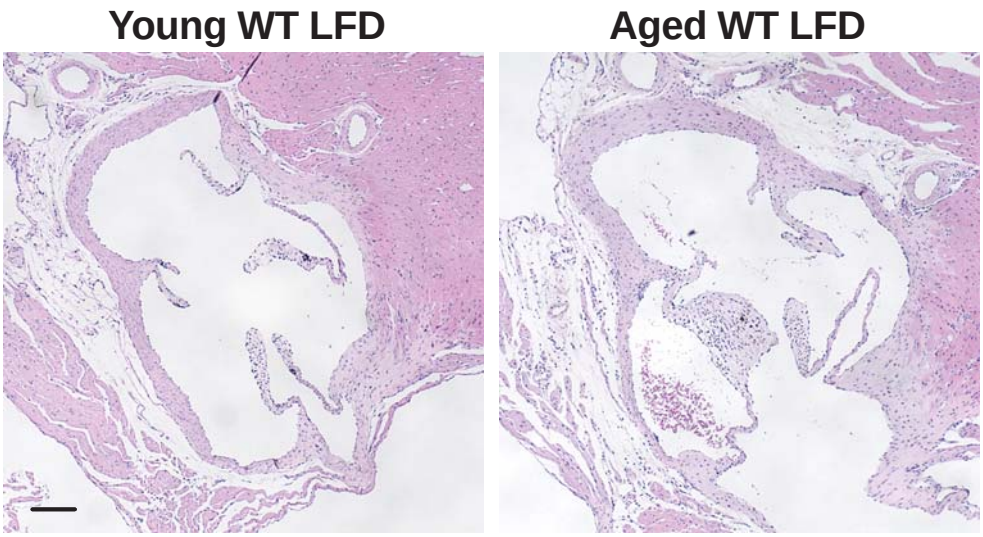

Online Figure XII: WT young or aged mice maintained on LFD do not exhibit atherosclerotic lesions. Aortic root sections were harvested and stained via H and E. There is no evidence of atherosclerosis in either young or aged mice. Scale bar: 100μm. LFD=low-fat diet.

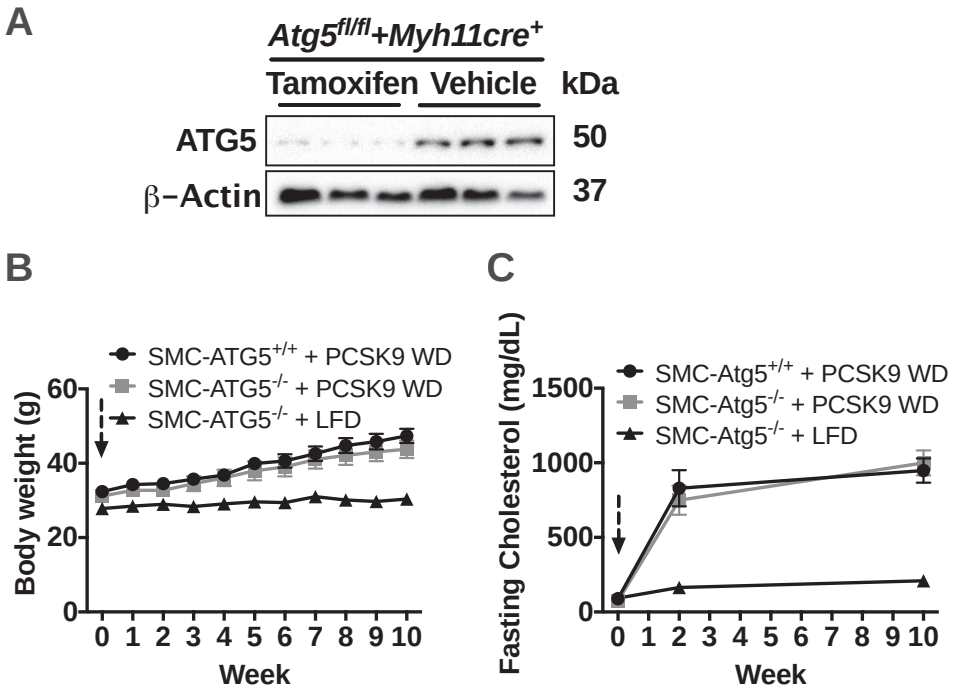

Online Figure XIII: Smooth muscle autophagy does not impact body weight gain or cholesterol level after PCSK9 transfection and during HFD feeding. (**A**) Aortic lysates from *Atg5$^{fl/fl}$Myh11-cre/ER^{T2}* mice treated with tamoxifen (ATG5$^{-/-}$) or vehicle (ATG5$^{+/+}$) were immunoblotted against ATG5 and β-actin (n=3 mice per group). (**B**) Body weight change of young tamoxifen-treated LFD-fed *Atg5$^{fl/fl}$Myh11-cre/ER^{T2}* mice, vehicle-treated PCSK9-HFD *Atg5$^{fl/fl}$Myh11-cre/ER^{T2}* mice, and tamoxifen-treated PCSK9-WD *Atg5$^{fl/fl}$Myh11-cre/ER^{T2}* mice (N=5-7 mice per group). Arrow indicates start of WD-feeding period. (**C**) Fasting cholesterol level (N=3-7 mice per group). Arrow indicates start of WD-feeding period. All results are presented as mean ±SEM. Mann-Whitney U-test. ATG5=autophagy protein 5, LFD=low-fat diet, PCSK9=proprotein convertase subtilisin/kexin 9, SMC=smooth-muscle cell, WD=western diet.

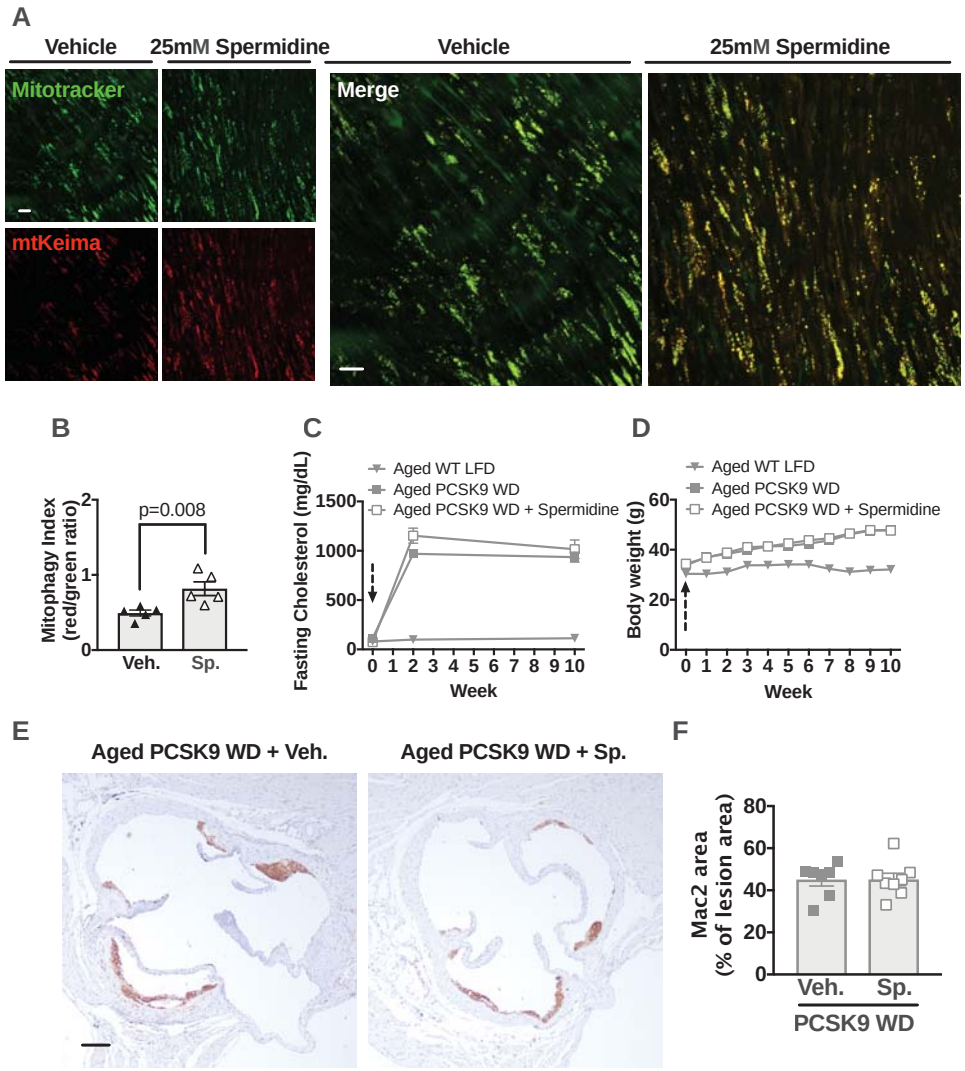

Online Figure XIV: Spermidine enhances mitophagy in aortas in tissue culture. Systemic spermidine treatment does not alter cholesterol levels or body weight. Spermidine does not impact macrophage numbers within atherosclerotic lesions of aged mice. (**A**) Aortas were harvested from young (4 months of age) mtKiema mice (see detailed methods). Aortas were incubated with mitotracker green or 25mM spermidine. The mitotracker green signal (488nm excitation) and mtKeima red signal (561nm excitation) were assessed by fluorescence microscopy (see detailed methods) and the ratio of 561:488 (mitophagy index) is shown in (**B**). Scale bar: 10μm (**C**) Aged WT mice were administered spermidine in drinking water during the 10-week WD feeding period after PCSK9-AAV. Low-fat diet fed mice were not administered spermidine. Fasting cholesterol levels of aged WT-LFD mice and aged PCSK9-WD mice administered spermidine or vehicle (N=4 aged WT-LFD, 3 aged PCSK9-WD, 7 aged PCSK9-WD + spermidine). Arrow indicates start of WD-feeding period. (**D**) Body weight change of young and aged PCSK9-WD mice and young and aged PCSK9-WD mice administered spermidine. Arrow indicates start of WD-feeding period. (**E**) $Mac2^{+}$ staining of aged mice that were administered 10-week WD feeding period after PCSK9-AAV and either treated with spermidine in drinking water or vehicle control. Scale bar: 100μm. For **C** and **D**, N=3 aged WT-LFD, 10 aged PCSK9-WD, 10 PCSK9-WD + spermidine. Each data point represents a biological replicate. All results are presented as mean ±SEM. LFD=low-fat diet, PCSK9=proprotein convertase subtilisin/kexin 9, WD=western diet.

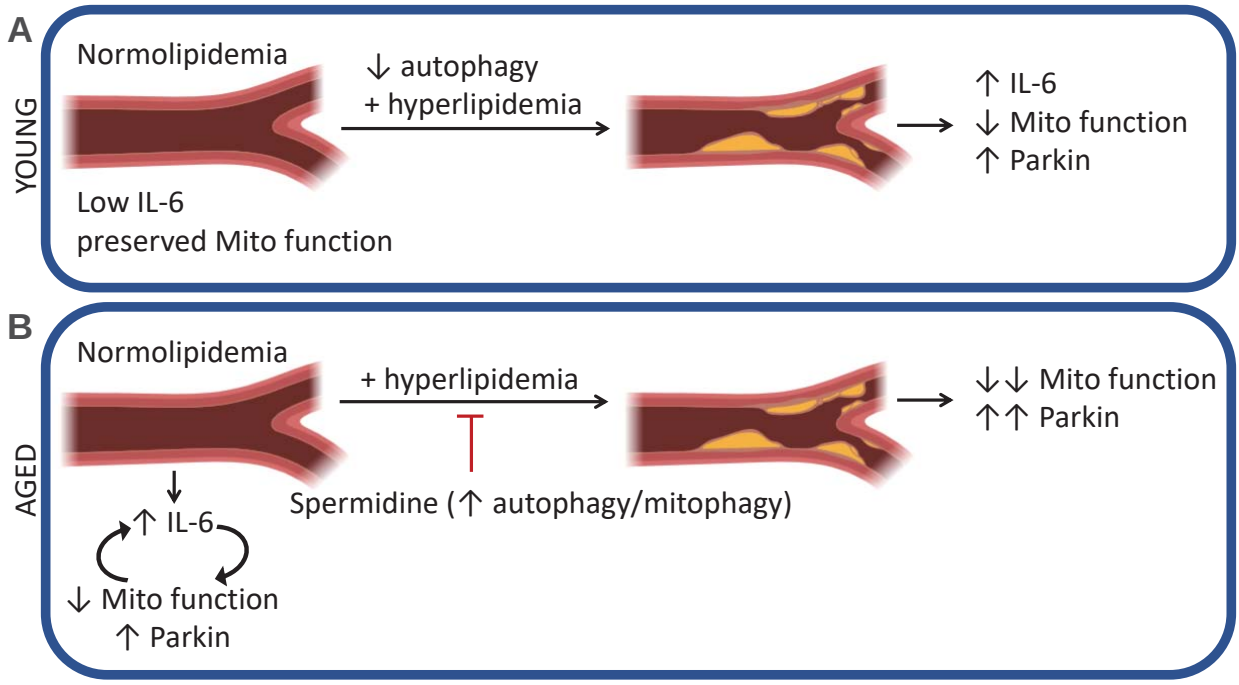

Online Figure XV: Pathways of mitochondrial dysfunction in young and aged aortas. (**A**) In young normolipidemic hosts, the aorta displays low IL-6 levels, normal mitochondrial function. Disabling smooth muscle autophagy (insult #1) with hyperlipidemia (insult #2) results in increased IL-6, elevated Parkin levels and mitochondrial dysfunction with increased atherogenesis. (**B**) Aged normolipidemic hosts display mitochondrial dysfunction, elevated IL-6 and increased Parkin within the aorta. Hyperlipidemia exacerbates these in aged hosts and spermidine attenuates this.

Supplemental Material References

1. Hara T, Nakamura K, Matsui M, Yamamoto A, Nakahara Y, Suzuki-Migishima R, Yokoyama M, Mishima K, Saito I, Okano H and Mizushima N. Suppression of basal autophagy in neural cells causes neurodegenerative disease in mice. *Nature*. 2006;441:885-9.
2. Sun N, Yun J, Liu J, Malide D, Liu C, Rovira Ilsa I, Holmström Kira M, Fergusson Maria M, Yoo Young H, Combs Christian A and Finkel T. Measuring In Vivo Mitophagy. *Molecular Cell*. 2015;60:685-696.
3. Miller RA and Chrisp C. Lifelong treatment with oral DHEA sulfate does not preserve immune function, prevent disease, or improve survival in genetically heterogeneous mice. *J Am Geriatr Soc*. 1999;47:960-6.
4. Du W, Wong C, Song Y, Shen H, Mori D, Rotllan N, Price N, Dobrian AD, Meng H, Kleinstein SH, Fernandez-Hernando C and Goldstein DR. Age-associated vascular inflammation promotes monocytosis during atherogenesis. *Aging Cell*. 2016;15:766-777.
5. Song Y, Shen H, Schenten D, Shan P, Lee PJ and Goldstein DR. Aging Enhances the Basal Production of IL-6 and CCL2 in Vascular Smooth Muscle Cells. *Arterioscler Thromb Vasc Biol*. 2012;1:103-9.
6. Bjorklund MM, Hollensen AK, Hagensen MK, Dagnaes-Hansen F, Christoffersen C, Mikkelsen JG and Bentzon JF. Induction of atherosclerosis in mice and hamsters without germline genetic engineering. *Circ Res*. 2014;114:1684-9.
7. Eisenberg T, Abdellatif M, Schroeder S, Primessnig U, Stekovic S, Pendl T, Harger A, Schipke J, Zimmermann A, Schmidt A, Tong M, Ruckenstuhl C, Dammbrueck C, Gross AS, Herbst V, Magnes C, Trausinger G, Narath S, Meinitzer A, Hu Z, Kirsch A, Eller K, Carmona-Gutierrez D, Buttner S, Pietrocola F, Knittelfelder O, Schrepfer E, Rockenfeller P, Simonini C, Rahn A, Horsch M, Moreth K, Beckers J, Fuchs H, Gailus-Durner V, Neff F, Janik D, Rathkolb B, Rozman J, de Angelis MH, Moustafa T, Haemmerle G, Mayr M, Willeit P, von Frieling-Salewsky M, Pieske B, Scorrano L, Pieber T, Pechlaner R, Willeit J, Sigrist SJ, Linke WA, Muhlfeld C, Sadoshima J, Dengjel J, Kiechl S, Kroemer G, Sedej S and Madeo F. Cardioprotection and lifespan extension by the natural polyamine spermidine. *Nat Med*. 2016;22:1428-1438.
8. Paigen B, Morrow A, Holmes PA, Mitchell D and Williams RA. Quantitative assessment of atherosclerotic lesions in mice. *Atherosclerosis*. 1987;68:231-40.
9. Daugherty A, Tall AR, Daemen M, Falk E, Fisher EA, Garcia-Cardena G, Lusis AJ, Owens AP, 3rd, Rosenfeld ME, Virmani R, American Heart Association Council on Arteriosclerosis T, Vascular B and Council on Basic Cardiovascular S. Recommendation on Design, Execution, and Reporting of Animal Atherosclerosis Studies: A Scientific Statement From the American Heart Association. *Arterioscler Thromb Vasc Biol*. 2017;37:e131-e157.
10. Fernandez-Hernando C, Ackah E, Yu J, Suarez Y, Murata T, Iwakiri Y, Prendergast J, Miao RQ, Birnbaum MJ and Sessa WC. Loss of Akt1 leads to severe atherosclerosis and occlusive coronary artery disease. *Cell Metab*. 2007;6:446-57.
11. Gnaiger E, Kuznetsov AV, Schneeberger S, Seiler R, Brandacher G, Steurer W and Margreiter R. Mitochondria in the Cold. *Life in the Cold*. 2000:431-442.
12. Frayn KN. Calculation of substrate oxidation rates in vivo from gaseous exchange. *J Appl Physiol Respir Environ Exerc Physiol*. 1983;55:628-34.